Mechanisms of Li^+ transport in garnet-type cubic $Li_{3+x}La_3M_2O_{12}$ (M = Te, Nb, Zr)

Ming Xu,[1,2] Min Sik Park,[1,*] Jae Myung Lee,[1] Tae Young Kim,[1] Young Sin Park,[1] and Evan Ma[2]
[1]*Battery Group, Samsung Advanced Institute of Technology, Yongin 446-712, Republic of Korea*
[2]*Department of Materials Science and Engineering, Johns Hopkins University, Baltimore, Maryland 21218, USA*
(Received 28 December 2011; published 29 February 2012)

We have studied a promising lithium-ion conductor, garnet-type cubic Li oxides, at various Li concentrations. The *ab initio* calculations performed on these materials revealed two distinct mechanisms of Li-ion transport, with very different energy barriers and a strong dependence on Li distribution. Our findings explain the origin of the vastly varying ionic conductivities at different Li concentrations and suggest possible principles to improve such materials for solid-state electrolyte applications.

DOI: 10.1103/PhysRevB.85.052301 PACS number(s): 66.30.Dn, 71.15.Mb, 82.47.Aa

Materials which are insulating to electrons but conductive to ions are potential candidates for electrolytes in batteries.[1] So far, the market-leading Li-ion conducting electrolytes are made hybrid: The polymeric Li oxides are immersed in a plasticizing organic solvent. Such liquid-ion conductors come with many issues, e.g., possible explosivity, limitations for miniaturization, and environmental contamination if not recycled properly. In this respect, inorganic solid-state Li-ion conductors would become good substitutions for the liquid ones, not only because they are safe and nontoxic, but also owing to their easy preparation and low cost.[2] However, the ionic conductivity (σ) of such solid-state ion conductors is not as satisfactory as its competitors. Hence, there is a pressing need for solid-state electrolytes with a high ionic conductivity, for next-generation Li-ion batteries.

Recently, garnet-type Li oxides came to the attention of researchers,[3,4] with the stoichiometric composition of $Li_{3+x}La_3M_2O_{12}$ (LLM), where M denotes various metallic or metalloid cations and x is tuned according to the charge balance (in some cases, La can also be replaced for easy preparation purposes). The single-crystal x-ray diffraction (XRD) experiments reported on the cubic (c) and the tetragonal (t) structures of LLM under ambient conditions, with c-LLM usually having higher ionic conductivity than t-LLM.[4,5] The typical ionic conductivity was found to be as high as 10^{-4} S/cm at room temperature in c-$Li_7La_3Zr_2O_{12}$,[5] making it a desirable candidate for a solid-state electrolyte. However, the structural complexity in this garnet-type crystal hampers the understanding of the mechanism of Li-ion transport and also adds difficulty to the improvement of such electrolytes. For example, the distribution of Li ions (Li^+) in such materials, as well as the primary factor that controls the ionic conductivity in these materials, is still unknown. In this Brief Report, we use *ab initio* tools to study three prototypes of c-LLM: $Li_3La_3Te_2O_{12}$ (LLT, $x = 0$), $Li_5La_3Nb_2O_{12}$ (LLN, $x = 2$), and $Li_7La_3Zr_2O_{12}$ (LLZ, $x = 4$). These three compositions with different Li concentrations have distinctly different ionic conductivities ($\sigma_{LLT} \sim 0$ as LLT behaves almost identically as other available garnet-type Li_3 compositions in our simulations, $\sigma_{LLN} \sim 10^{-6}$ S/cm, $\sigma_{LLZ} \sim 10^{-4}$ S/cm),[5–7] although they are in the same garnet frame. Our simulations have unraveled the stable (relaxed) atomic structures of these three Li oxides, mapped out the Li migration paths that explain the influence of Li concentration on the structure and the activation energy, and suggested a principle that can potentially improve the ionic conductivity of such garnet-type materials.

The *ab initio* calculations were performed at 0 K by using the Vienna *ab initio* simulation package (VASP) code,[8] based on the density functional theory (DFT). The projector augmented-wave (PAW) method[9] with the generalized gradient approximation (GGA)[10] for the exchange-correlation functional was employed. Supercells containing 160, 176, and 192 atoms were used in our simulations for LLT, LLN, and LLZ, respectively (eight times the number of atoms in each formula). After we had determined the stable structures, the nudged elastic band (NEB) method[11] was applied to find the minimum energy path (MEP) of Li migration. Several possible transition points ("images") were first interpolated between the initial and the final states, and the elastic band method added suppositional spring forces between neighboring images to maintain similar intervals between them. The calculations are convergent when the MEP is found.

The stable atomic structure of c-LLM is a key to understanding the mechanism of Li transport. The c-LLM has a garnet-type structure, belonging to the space group Ia-$3d$ (No. 230).[12–14] In this frame, M and La ions are located in the centers of octahedral MO_6 (24c sites) and dodecahedral LaO_8 (16a sites), respectively. On the other hand, there are two kinds of sites to accommodate Li ions, the tetrahedral sites [Li(1), 24d sites] and the octahedral sites [Li(2), 48g/96h sites]. The Li(2) sites are enclosed by the triangle faces of two neighboring Li(1) sites, so each Li(1) site has four neighboring Li(2) sites. In total, there are 24 Li(1) sites and 48 Li(2) sites in each supercell. The corresponding atomic structure and the Wyckoff positions of Li ions are shown in Fig. 1. Experimentally, Li ions are supposed to partially occupy both sites, with the leftover vacant sites that enable the hopping of the mobile ions. However, consensus has not been reached on the exact Li occupancy on these two different sites, owing to the limitations of XRD or nuclear magnetic resonance (NMR).[15] So far, it is reported[13] that Li(1) sites are more favorable than Li(2) sites, suggesting high occupancy in Li(1) sites.

Our calculations start from those unrelaxed structures in which Li(1) sites have high occupancy. In addition to the well-defined La, M, and O positions, 24 Li ions are filled in 24 Li(1) sites so that they are fully occupied, and the rest of the Li ions (0, 16, 32 for LLT, LLN, and LLZ, respectively) are randomly distributed in the center of 48 Li(2) sites. All ions are allowed

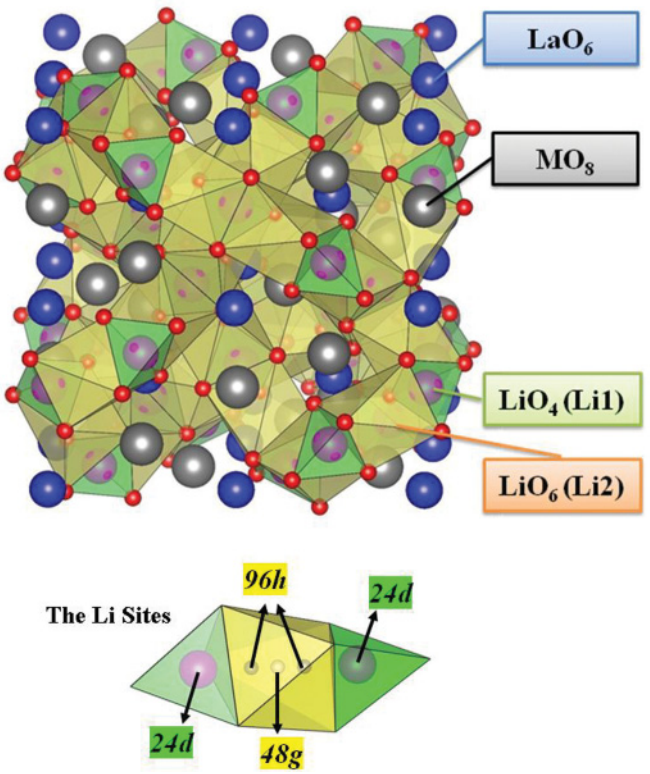

FIG. 1. (Color online) The atomic structure of garnet-type *c*-LLM. The green (dark gray) polyhedrons are tetrahedral Li(1) sites and the yellow (light gray) ones are octahedral Li(2) sites. Each Li(1) site is enclosed by four neighboring Li(2) sites and each Li(2) site connects two neighboring Li(1) sites. The occupancy of Li(1) and Li(2) sites depends on the Li concentration. The snapshot below is the Wyckoff positions that the Li ions could possibly be located. The centers of Li(1) and Li(2) sites are noted as 24*d* and 48*g* sites, respectively, and the 96*h* sites are slightly displaced off the 48*g* sites but they are still inside the Li(2) octahedra.

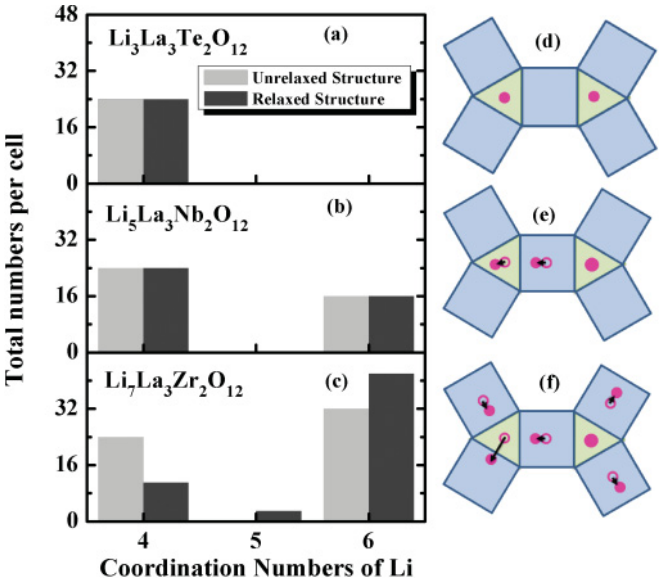

FIG. 2. (Color online) (a)–(c) The coordination numbers (CN) of Li ions in LLT, LLN, and LLZ. CN = 4, 5, 6 represent Li ions that are inside tetrahedral sites [Li(1) sites], near the tetrahedral-octahedral borders [Li(1)-Li(2) borders], and inside octahedral sites [Li(2) sites], respectively. The unrelaxed structures mean all Li(1) sites are occupied and the remaining Li ions randomly occupy the Li(2) sites, while the stable structures are obtained by relaxing the proposed ones. (d)–(f) 2D schematics of the Li positions in three corresponding compositions. Triangular and square sites denote Li(1) and Li(2) sites, and the open and solid circles are proposed and stable positions of Li ions, respectively (the arrows indicate the direction of displacement).

to move so as to search for the lowest-energy positions. After the relaxation, we analyze the coordination numbers (CN) of Li^+ in the stable phase (cutoff =3 Å, which is longer than the nearest Li-O bond length but shorter than the second-nearest distance). The calculated results are shown in Fig. 2, together with the two-dimensional (2D) schematics of typical local configurations of Li^+ in the three compositions.

The relaxed structure of LLT ($x = 0$) is almost the same as the unrelaxed one, with all Li ions occupying the tetrahedral Li(1) sites and no ion found in the octahedral Li(2) sites [Figs. 2(a) and 2(d)]. The absence of Li(2) neighbors ensures the stability of the Li(1) sites. And even for LLN ($x = 2$) in which the occupancy of Li(2) sites is relatively low, the tetrahedral Li(1) sites are still energetically preferred for Li ions [Fig. 2(b)]. However, a detailed analysis of the Li positions reveals that most of them have displaced off their original central 48*g* sites, approaching the 96*h* sites [see Fig. S1a in the Supplemental Material[16]). This displacement results from the short Li $\cdots$ Li distance ($\sim$1.9 Å) in the unrelaxed structure, which could generate a large Coulombic repulsion to push them apart, and the equilibrium Li $\cdots$ Li intervals (2.2–2.4 Å)[14] are reached after the relaxation (see Fig. S1d in the Supplemental Material[16]). Despite the minor off-site displacements, no Li ions move out of the initial polyhedral boxes, and such displacements have no preferred directions, resulting in a disordered distribution in both Li sites.[14]

The continuous increase of the Li concentration, however, will greatly undermine the stability of Li(1) sites. In LLZ ($x = 4$), the Li distribution in the stable structure is totally different from what is proposed [that all Li(1) sites and 2/3 Li(2) sites are occupied]. It is observed that when two or more Li(2) ions move simultaneously toward their common Li(1) neighbor, this Li(1) ion will be pushed to the Li(1)-Li(2) border and further into the empty Li(2) sites nearby [Fig. 2(f)]. The analysis of CN [Fig. 2(c)], the displacement (see Fig. S1b in the Supplemental Material[16]), and the resulting bifurcation of Li-O bonds (see Fig. S1e in the Supplemental Material[16]) clearly show this trend, in which more than half of the tetrahedral sites have been left empty and the occupancy of the Li(2) sites increase to 90% [Fig. 2(c)], which is consistent with the recent experimental findings.[17] Another possible configuration in which both 96*h* sites in a single octahedron could be occupied was proposed in Ref. 13. We exclude this configuration by a simulation showing that it is rather unfavorable (see Fig. S2 in the Supplemental Mateiral[16]).These structural features shown in Fig. 2 result in different and even contrasting Li behaviors in the ion transport. In LLT, due to the very low occupancy ($\sim$0) of Li(2) sites, the only possible path for the Li migration is to activate it from the tetrahedral site to the neighboring octahedral site. The energy cost of this Li^+ migration is as

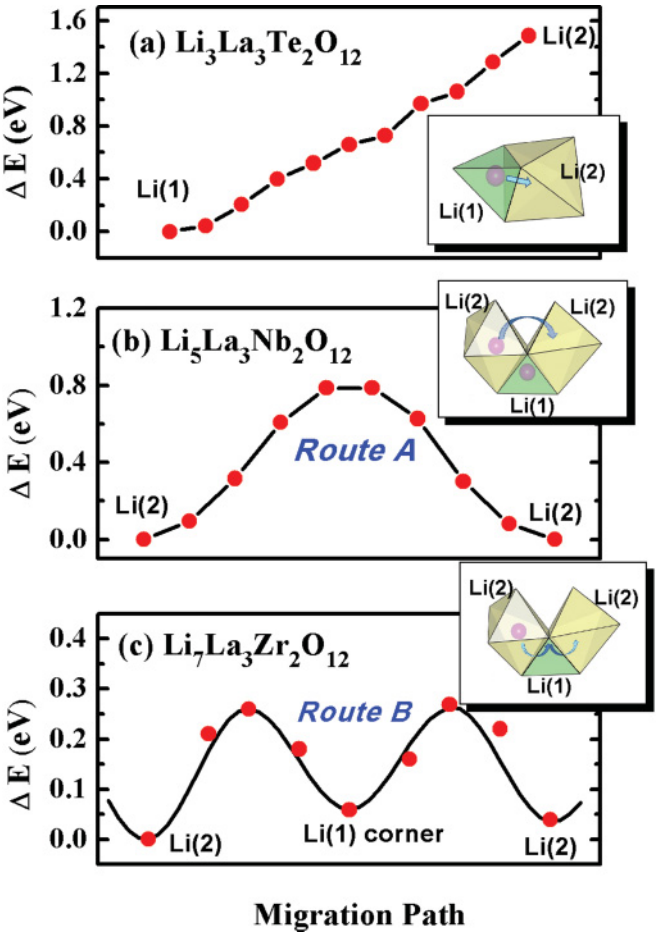

FIG. 3. (Color online) (a) The energy cost to move one Li^+ ion from the Li(1) site to the neighboring Li(2) site in LLT. (b), (c) Two predominant mechanisms of Li migration, (a) *Route A* in LLN and (b) *Route B* in LLZ. The energy barriers are calculated to be 0.8 and 0.26 eV, respectively. The dots are the calculated points and the lines are the energy of the extrapolated migration paths. The arrows in the insets (b) and (c) indicate these two distinct migration paths.

high as 1.5 eV [Fig. 3(a)], making it impossible to take place at room temperature. Furthermore, the octahedral Li(2) sites are not even metastable, such that any Li^+ appearing at this site will be immediately dragged back to the neighboring empty tetrahedral Li(1) site. In other words, these stable tetrahedral Li(1) sites act as energetic traps to keep Li^+ immobile in these positions. Thus the lack of mobile Li^+ explains why the ionic conductivity of LLT (or any other garnet-type Li oxides with $x = 0$) can hardly be detected at room temperature.[6] It is noted that the high occupancy in the Li(1) sites holds true only for the low Li concentration case [on average, less than two octahedral Li(2) neighbors for each tetrahedral Li(1) ion].

Similar to LLT, the Li(1) sites are still stable in LLN, but the additional Li ions now occupy 1/3 of the Li(2) sites in addition to Li(1) sites. The coexistence of mobile Li ions and vacancies in Li(2) sites makes ion transport possible. The NEB calculation shows that the MEP of the Li migration in LLN is via the interstice between neighboring Li(2)-Li(2) sites, bypassing their common tetrahedral Li(1) neighbor [*Route A*, shown in Fig. 3(b)]. The energy needed for the mobile Li^+ to climb over the in-between interstice is demonstrated to be relatively high, 0.8 eV in our calculations, even higher than the "bottlenecks", the triangular faces enclosed by three oxygen atoms. This calculated energy barrier for *Route A* is higher than the experimental activation energies (0.4–0.6 eV, $x = 2$),[18] but such a discrepancy is not unexpected of DFT/NEB simulations and will be taken into account in the estimation of bulk ionic conductivity later.

In the case of LLZ, the mechanism of Li migration becomes intriguing owning to the complexity of its structure. However, it is found in our model that only 10% of the Li(2) sites are vacant and they mainly concentrate around the empty Li(1) sites. This narrows down the search for a Li migration path because these vacant Li(2) sites should be involved in the ion hopping. In light of this, the Li migration is most likely to take place between the Li(2) sites adjacent to the empty Li(1) sites. The NEB calculation shows that, unlike *Route A* in the LLN, the mobile Li(2) ion will follow a new path [*Route B*, shown in Fig. 3(c)], in which it moves through the Li(1)-Li(2) border (the shared triangular faces), sticking around briefly at the corner of Li(1) site (which is also now a local minimum energy position), then climbing over the other Li(1)-Li(2) border and finally arriving at the vacant Li(2) site. The bottleneck is at the shared triangular faces of Li(1) and Li(2) sites, and the resultant main energy barrier for such a migration path is calculated to be 0.26 eV, which is much lower than the energy cost of *Route A*. This low-energy barrier explains why LLZ exhibits rather high ionic conductivity.

Our above studies clearly show that the Li concentration (the x value) in these garnet-type ion conductors will redistribute the location of Li^+ over the Li(1) and Li(2) sites. As a result, two distinct ion migration paths (*Routes A* and *B*) could result, according to different scenarios of local Li^+ ion environments, with *Route B* having a much lower-energy barrier than *Route A*, indicating higher bulk ionic conductivity if more mobile Li ions take *Route B* (the energy barrier of a designated path is almost independent of the Li concentrations and configurations in our simulations, e.g., *Route A* has a barrier of ~0.8 eV in all garnet-type compositions). However, in LLN ($x = 2$) or LLZ ($x = 4$) or materials with other Li concentrations ($x = 2$–4), both migration routes should be involved, and the probability of the *Route B* transport is much higher in the large Li concentration materials (x toward 4) than that in cases of low Li concentration ($x \leqslant 2$). Therefore, the bulk ionic conductivity (σ_{bulk}, given no grain boundary included) of a garnet-type ion conductor is primarily dependent on the Li concentrations, while other factors such as different dopant elements or lattice parameters are only secondary contributors. This finding is consistent with the reported measurement of the bulk ionic conductivities for different compositions at room temperature (see Fig. 4 and Table S1 in the Supplemental Material[16]), which clearly shows that such garnet-type materials with the same Li concentration usually have the same order of σ_{bulk}, regardless of different dopant elements.[5–7,18–26] The estimated ionic conductivity based on our calculated vacancy occupancies and migration energy barriers is compared with the experimental data in Fig. 4, using the equation based on the random-walk theory:[27]

$$\sigma = \frac{\sigma_0}{T} \exp\left(-\frac{E_a}{kT}\right), \tag{1}$$

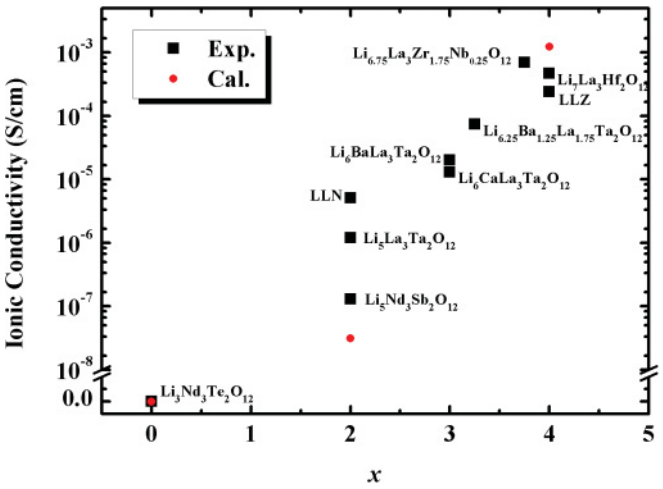

FIG. 4. (Color online) The bulk ionic conductivities of various garnet-type Li oxides measured at room temperature (Refs. 5–7 and 18–26), together with the calculated ones based on our simulations.

where σ_0 is the preexponential factor which is closely related to the vacancy occupancies, and E_a is the activation energy. Considering the error margin of the NEB method in calculating the energy barrier, we use $E_a = 0.6$ eV and $E_a = 0.3$ eV for $x \sim 2$ and $x \sim 4$ cases, respectively, and the vacancy occupancies are estimated using the CN of Li ions.

Our study has the following implications for the improvement of these garnet-type ion conductors. First, owing to the redistribution of Li ions in LLZ ($x = 4$), the occupancy of mobile Li(2) sites already reaches 90%. Such a high occupancy, although helpful to promote more *Route B* transport, leaves insufficient vacancies for the ion migration. Therefore, a further increase of Li concentration is not advised, and an optimized Li/vacancy ratio is required so that it possesses enough empty room to accept the hopping Li^+, as well as to minimize the *Route A* transport which has a high-energy barrier. An example of this attempt is the Nb-doped LLZ ($x = 3.75$) which exhibits even higher σ_{bulk} than the undoped LLZ ($x = 4$),[25] as listed in Fig. 4 and Table S1.[16] Second, the dopant could increase σ_{bulk} by mediating the Li concentrations, but itself has a minor influence on the energy barrier of the ion migration. Meanwhile, the lattice parameters owing to different dopants are varied within 1%, too small to affect the energy barrier at the bottleneck, given the same Li concentration. Therefore, apart from the mediation of Li concentrations, a good dopant should be able to reduce the grain-boundary resistance[18,28] (ρ_{gb}, the resistance that ions may encounter when traveling through the grain boundary), prevent electronic transport, and ensure low cost and easy preparation for possible commercialization.

To conclude, we systematically studied three garnet-type ion conductors ($Li_{3+x}La_3M_2O_{12}$, $x = 0, 2, 4$) using *ab initio* tools. The structure analysis shows that Li ions have high occupancy at tetrahedral sites for $x \leqslant 2$ cases, but this tetrahedral occupancy is destabilized and reduced to ~50% in $Li_7La_3Zr_2O_{12}$ ($x = 4$) while the occupancy of mobile Li ions in octahedral sites increases to 90%. Two distinct migration paths, which have different energy barriers, are discovered in these materials. The high-energy path prevails in the low Li concentration ($x \leqslant 2$) compositions, while the high Li concentration (x toward 4) enables the transport to primarily adopt the low-energy path. The combination of these two migration paths, which depends strongly on the Li concentration, characterizes the ion transport in these garnet-type ion conductors, leading to their pronounced differences in bulk ionic conductivities.

The authors are grateful to the supercomputing center in SAIT for providing computational facilities.

*ms91.park@samsung.com

[1] M. Park, X. Zhang, M. Chung, G. B. Less, and A. M. Sastry, J. Power Sources **195**, 7904 (2010).
[2] E. Quartarone and P. Mustarelli, Chem. Soc. Rev. **40**, 2525 (2011).
[3] P. Knauth, Solid State Ionics **180**, 911 (2009).
[4] E. J. Cussen, J. Mater. Chem. **20**, 5167 (2010).
[5] R. Murugan, V. Thangadurai, and W. Weppner, Angew. Chem., Int. Ed. **46**, 7778 (2007).
[6] M. P. O'Callaghan, A. S. Powell, J. J. Titman, G. Z. Chen, and E. J. Cussen, Chem. Mater. **20**, 2360 (2008).
[7] V. Thangadurai, H. Kaack, and W. J. F. Weppner, J. Am. Ceram. Soc. **86**, 437 (2003).
[8] G. Kresse and J. Furthmüller, Comput. Mater. Sci. **6**, 15 (1996).
[9] P. E. Blöchl, Phys. Rev. B **50**, 17953 (1994).
[10] J. P. Perdew, K. Burke, and M. Ernzerhof, Phys. Rev. Lett. **77**, 3865 (1996).
[11] G. Mills, H. Jónsson, and G. K. Schenter, Surf. Sci. **324**, 305 (1995).
[12] R. Murugan, W. Weppner, P. Schmid-Beurmann, and V. Thangadurai, Mater. Sci. Eng. B **143**, 14 (2007).
[13] J. Awaka, A. Takashima, K. Kataoka, N. Kijima, Y. Idemoto, and J. Akimoto, Chem. Lett. **40**, 60 (2011).
[14] E. J. Cussen, Chem. Commun. 412 (2006).
[15] L. van Wüllen, T. Echelmeyer, H.-W. Meyer, and D. Wilmer, Phys. Chem. Chem. Phys. **9**, 3298 (2007).
[16] See Supplemental Material at http://link.aps.org/supplemental/10.1103/PhysRevB.85.052301 for relaxed Li-ion positions and experimental ionic conductivities of some typical garnet-type electrolytes.
[17] H. Xie, J. A. Alonso, Y. T. Li, M. T. Fernandez-Diaz, and J. B. Goodenough, Chem. Mater. **23**, 3587 (2011).
[18] S. Narayanan and V. Thangadurai, J. Power Sources **196**, 8085 (2011).
[19] M. P. O'Callaghan, D. R. Lynham, E. J. Cussen, and G. Z. Chen, Chem. Mater. **18**, 4681 (2006).
[20] E. J. Cussen, T. W. S. Yip, G. Oneill, and M. P. Ocallaghan, J. Solid State Chem. **184**, 470 (2011).
[21] J. Percival, E. Kendrick, and P. R. Slater, Mater. Res. Bull. **43**, 765 (2008).
[22] J. Awaka, N. Kijima, Y. Takahashi, H. Hayakawa, and J. Akimoto, Solid State Ionics **180**, 602 (2009).
[23] V. Thangadurai and W. Weppner, Adv. Funct. Mater. **15**, 107 (2005).

[24]R. Murugan, V. Thangadurai, and W. Weppner, Ionics **13**, 195 (2007).
[25]S. Ohta, T. Kobayashi, and T. Asaoka, J. Power Sources **196**, 3342 (2011).
[26]T. Zaiß, M. Ortner, R. Murugan, and W. Weppner, Ionics **16**, 855 (2010).
[27]P. Maldonado-Manso, E. R. Losilla, M. Martinez-Lara, M. A. G. Aranda, S. Bruque, F. E. Mouahid, and M. Zahir, Chem. Mater. **15**, 1879 (2003).
[28]S. Kumazaki, Y. Iriyama, K. H. Kim, R. Murugan, K. Tanabe, K. Yamamoto, T. Hirayama, and Z. Ogumi, Electrochem. Commun. **13**, 509 (2011).